# Site Selectivity in Pd-Catalyzed Reactions of α-Diazo-α-(methoxycarbonyl)acetamides: Effects of Catalysts and Substrate Substition in the Synthesis of Oxindoles and β-Lactams

**Daniel Solé [1,\*]** ![ORCID], **Ferran Pérez-Janer [1], Arianna Amenta [1], M.-Lluïsa Bennasar [1] and Israel Fernández [2,\*]**

[1] Laboratori de Química Orgànica, Facultat de Farmàcia i Ciències de l'Alimentació, Universitat de Barcelona, Av. Joan XXIII 27-31, 08028 Barcelona, Spain; ferranperez1@hotmail.com (F.P.-J.); amenta.arianna@gmail.com (A.A.); bennasar@ub.edu (M.-L.B.)

[2] Departamento de Química Orgánica I and Centro de Innovación en Química Avanzada (ORFEO-CINQA), Facultad de Ciencias Químicas, Universidad Complutense de Madrid, 28040 Madrid, Spain

[\*] Correspondence: dsole@ub.edu (D.S.); israel@quim.ucm.es (I.F.); Tel.: +34-934024540 (D.S.)

![check for updates]

**Abstract:** The Pd-catalyzed intramolecular carbene C–H insertion of α-diazo-α-(methoxycarbonyl)acetamides to prepare oxindoles as well as β-lactams was studied. In order to identify what factors influence the selectivity of the processes, we explored how the reactions are affected by the catalyst type, using two oxidation states of Pd and a variety of ligands. It was found that, in the synthesis of oxindoles, $((IMes)Pd(NQ))_2$ can be used as an alternative to $Pd_2(dba)_3$ to catalyze the carbene $C_{Ar}sp^2$–H insertion, although it was less versatile. On the other hand, it was demonstrated that the $Csp^3$–H insertion leading to β-lactams can be effectively promoted by both Pd(0) and Pd(II) catalysts, the latter being most efficient. Insight into the reaction mechanisms involved in these transformations was provided by DFT calculations.

## 1. Introduction

In recent years, the development of new methodologies for the selective functionalization of unactivated C–H bonds has become a very active area of research [1,2]. As part of this exciting field, the transition metal-catalyzed intramolecular carbene C–H insertion by decomposition of α-diazocarbonyl compounds has emerged as a powerful methodology for the construction of carbocyclic and heterocyclic frameworks [3–8]. A number of transition metal complexes have been used as effective catalysts to generate reactive metallacarbenes starting from α-diazocarbonyl compounds [9–16]. Among them, rhodium(II) [17,18], copper(I) [19,20], and more recently ruthenium(II) catalysts [21–27] have been proven to be especially useful for the development of highly selective carbene C–H insertion methodologies via a variety of reaction modes. Interestingly, palladium, one of the most commonly employed metals in homogeneous catalysis, remains underexploited in this type of carbene C–H insertion processes. Thus, while the effectiveness of palladium complexes in catalyzing carbene C–H insertion reactions from α-diazo carbonyl compounds was demonstrated some time ago [28], their use has been restricted to a couple of examples of insertion into $C_{Ar}sp^2$–H bonds [29–31]. This fact is highly surprising if we take into account the great success of palladium catalysis in cross-coupling reactions of diazo compounds with organic halides, pseudohalides, or arylboronic acids [32–35] and

that the palladium-catalyzed cyclopropanation of olefins with diazomethane is a widely used synthetic methodology [36].

The longstanding research on transition metal-catalyzed carbene C–H insertion has generated an extensive literature on the use of dirhodium(II) catalysts to promote the intramolecular C–H insertion of $\alpha$-diazoacetamides [37,38], as the insertion products, namely $\beta$- and $\gamma$-lactams as well as 2-oxindoles, are common scaffolds found in numerous natural products. In recent years, some ruthenium(II) catalysts have also been applied to promote this kind of C–H insertion process [21,22,25,39–43]. It has been shown that the site selectivity of these reactions not only depends on the type of diazocarbonyl compound but also is governed by conformational, steric, as well as electronic factors [44–46]. Moreover, some dramatic ligand effects have also been observed. For example, the use of carboxylate and, in particular, carboxamide ligands in dirhodium(II) catalysts has resulted in highly chemo-, regio- and stereoselective transformations [47,48] despite a variety of potentially competitive carbene-mediated processes (Scheme 1).
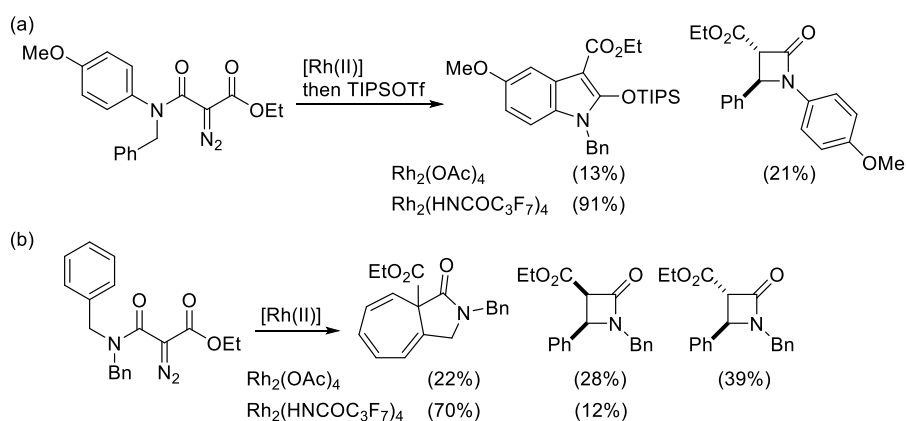


**Scheme 1.** Typical Rh(II)-catalyzed reactions of $\alpha$-diazoamides.

As part of our research program on the synthesis of nitrogen heterocycles, we have been exploring different ways to increase the versatility of palladium catalysis in C–C bond-forming reactions [49–51], for example, by controlling the ambiphilic character of the organopalladium intermediates in the intramolecular coupling reactions with carbonyl derivatives [52]. Continuing our search for methodologies to enhance the synthetic potential of organopalladium chemistry, we have also investigated the versatility of palladium as a catalyst for the carbene C–H insertion. In this context, we reported that palladium catalysts are able to promote $Csp^3$–H insertion of carbenes derived from $\alpha$-diazoesters to form pyrrolidines through intramolecular $Csp^3$–$Csp^3$ bond formation [53,54].

We have also demonstrated that the carbene $C_{Ar}sp^2$–H functionalization of $\alpha$-diazo-$\alpha$-(methoxycarbonyl)acetanilides to give oxindoles can also be promoted by using $Pd_2(dba)_3$ as the catalyst [55]. This allowed us to develop a one-pot methodology to prepare 3-(chloroethyl)oxindoles by means of a sequential C–H insertion/alkylation process (Equation (a) in Scheme 2). More recently, we have described the synthesis of $\beta$-lactams by Pd(II)-catalyzed carbene $Csp^3$–H insertion of $\alpha$-diazo-$\alpha$-(methoxycarbonyl)acetamides (Equation (b) in Scheme 2) [56].
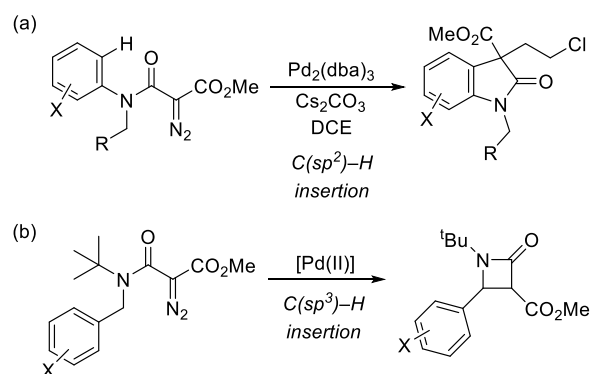
**Scheme 2.** Pd catalysts in C–H insertion reactions of α-diazo-α-(methoxycarbonyl)acetamides.

The aim of the current work was to gain more insight into the Pd-catalyzed carbene insertion reactions of α-diazo-α-(methoxycarbonyl)acetamides leading to oxindoles and β-lactams. In order to ascertain the factors governing the selectivity of the processes, we explored how the reactions are affected by the substituents on α-diazoacetamide and the type of catalyst, using complexes with two oxidation states of Pd and a variety of ligands (Scheme 3). Herein, we present a full account of our experimental and computational studies on the intramolecular insertion of α-diazo-α-(methoxycarbonyl)acetamides using Pd(0) and Pd(II) complexes, focused on identifying differences in the catalyst reactivities and selectivities.
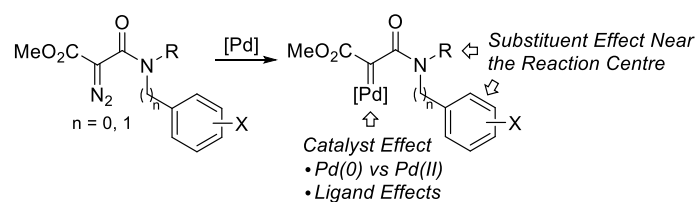


**Scheme 3.** Catalyst and substituent effects in Pd-catalyzed C–H insertion reactions of α-diazo-α-(methoxycarbonyl)acetamides.

## 2. Results and Discussion

The oxindole system is a common structural motif in pharmaceuticals and natural products, and the development of efficient procedures for their preparation is, therefore, of considerable interest [57–60].

Our previous studies on the carbene reactions of α-diazo-α-(methoxycarbonyl)acetanilides showed that, when using palladium catalysts, the C–H insertion giving the oxindole occurs selectively in the $C_{Ar}sp^2$–H rather than the $Csp^3$–H bonds (Equation (a) of Scheme 2) [55]. The optimization process with α-diazoacetanilide **1a** revealed that the carbene $C_{Ar}sp^2$–H insertion can be selectively promoted by both Pd(0) and Pd(II), the best result being obtained when using $Pd_2(dba)_3$ in the presence of $Cs_2CO_3$ in dichloroethane at reflux for 96 h, which afforded oxindole **2a** in 66% yield (Table 1, entry 1). However, this reaction required a high catalyst loading and long reaction time. All attempts to increase the efficiency of the Pd(0)-catalyzed reaction by adding different phosphine ligands failed, always resulting in a slower reaction rate.

In order to improve the efficiency of the carbene insertion of α-diazoacetanilide **1a**, in the present study, we tested some palladium catalysts bearing non-phosphine ligands. $(Pd(allyl)Cl)_2$ was first explored for the insertion/alkylation sequential process (Table 1, entries 2–3), but significant amounts of the starting material were recovered even after 60 h. In contrast, the use of $((IMes)Pd(NQ))_2$ required a notably shorter reaction time and lower catalyst loading (Table 1, entry 4).

**Table 1.** Palladium-catalyzed reactions of α-diazoamide **1a** [1].
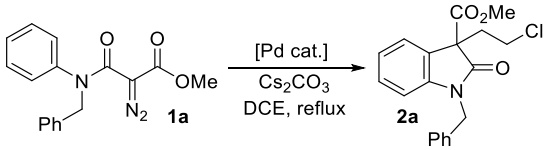


| Entry | Catalyst (mol%) | Time | Products (Yield (%)) [2] |
|-------|-----------------|------|--------------------------|
| 1 | Pd$_2$(dba)$_3$ (10) | 96 h [3] | **2a** (66) |
| 2 | (Pd(allyl)Cl)$_2$ (5) | 24 h | **1a/2a** (1:2.2) [4] |
| 3 | (Pd(allyl)Cl)$_2$ (5) | 60 h | **1a/2a** (1:5.5) [4] |
| 4 | ((IMes)Pd(NQ))$_2$ (4) | 24 h | **2a** (65) |

[1] All reactions were conducted with **1a** (0.2 mmol), catalyst (see table), and Cs$_2$CO$_3$ (1 equiv.) in dichloroethane (0.2 M) at reflux. Pd$_2$(dba)$_3$ = Tris(dibenzylideneacetone)dipalladium(0). ((IMes)Pd(NQ))$_2$ = 1,3-Bis(2,4,6-trimethylphenyl)imidazol-2-ylidene (1,4-naphthoquinone) palladium(0) dimer. [2] Isolated yield. [3] Cs$_2$CO$_3$ (2 equiv.). [4] ^{1}H-NMR ratio; yields were not quantified.

With these data in hand, we then explored the generality of the NHC-Pd(0) catalyst in the sequential C–H insertion/alkylation process, leading to 3-(chloroethyl)-3-(methoxycarbonyl)oxindoles. Table 2 gathers the results of the reactions of different α-diazoacetanilides (**1b–1j**) when using ((IMes)Pd(NQ))$_2$ as the catalyst and compares them with those previously obtained with Pd$_2$(dba)$_3$ [55].

**Table 2.** Palladium-catalyzed cyclization reactions of α-diazoamides **1b–1j**.
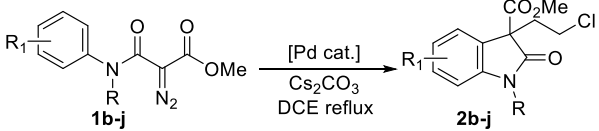


| Entry | Substance 1 | Catalyst [1,2] | Product (Yield (%)) [3] |
|-------|-------------|----------------|--------------------------|
| 1 | **1b** (R:Me) | Pd$_2$(dba)$_3$ | **2b** (71) |
| 2 | **1b** (R:Me) | ((IMes)Pd(NQ))$_2$ | **2b** (79) |
| 3 | **1c** (R:Et) | Pd$_2$(dba)$_3$ | **2c** (54) |
| 4 | **1c** (R:Et) | ((IMes)Pd(NQ))$_2$ | **2c** (78) |
| 5 | **1d** (R:*i*-Pr) | Pd$_2$(dba)$_3$ | **2d** (61) |
| 6 | **1d** (R:*i*-Pr) | ((IMes)Pd(NQ))$_2$ | **2d** (64) |
| 7 | **1e** (R:Ph) | Pd$_2$(dba)$_3$ [4] | **2e** (55) [5] |
| 8 | **1e** (R:Ph) | ((IMes)Pd(NQ))$_2$ | **2e** (35) |
| 9 | **1f** | Pd$_2$(dba)$_3$ | **2f** (23) [6] |
| 10 | **1f** | ((IMes)Pd(NQ))$_2$ | **2f** (0) [7] |
| 11 | **1g** (R$_1$:OMe) | Pd$_2$(dba)$_3$ | **2g** (36) |
| 12 | **1g** (R$_1$:OMe) | ((IMes)Pd(NQ))$_2$ | **2g** (76) |
| 13 | **1h** (R$_1$F) | Pd$_2$(dba)$_3$ | **2h** (64) |
| 14 | **1h** (R$_1$:F) | ((IMes)Pd(NQ))$_2$ | **2h** (39) [8] |
| 15 | **1i** (R$_1$:CO$_2$Me) | Pd$_2$(dba)$_3$ [4] | **2i** (22) |
| 16 | **1i** (R$_1$:CO$_2$Me) | ((IMes)Pd(NQ))$_2$ | **2i** (0) [9] |
| 17 | **1j** | Pd$_2$(dba)$_3$ [4] | **2j** (27) |
| 18 | **1j** | ((IMes)Pd(NQ))$_2$ | **2j** (23) [10] |

[1] Reactions were conducted with **1** (0.2 mmol), Pd$_2$(dba)$_3$ (10 mol%), and Cs$_2$CO$_3$ (1 equiv.) in dichloroethane (0.2 M) at reflux for 96 h. [2] Reactions were conducted with **1** (0.2 mmol), ((IMes)Pd(NQ))$_2$ (4 mol%), and Cs$_2$CO$_3$ (1 equiv.) in dichloroethane (0.2 M) at reflux for 48 h. [3] Isolated yield. [4] Catalyst loading: 15%. [5] 20% of unreacted **1e** was recovered. [6] ^{1}H-NMR analysis of the reaction mixture showed a 1:1 mixture of **1f** and **2f**. [7] **1f** was recovered. [8] ^{1}H-NMR analysis of the reaction mixture showed a 1:4.8 mixture of **1h** and **2h**. [9] Complex reaction mixture. [10] ^{1}H-NMR analysis of the reaction mixture showed a 1:1.5 mixture of **1j** and **2j**.

As can be seen in Table 2, like Pd$_2$(dba)$_3$, ((IMes)Pd(NQ))$_2$ also selectively promoted the carbene insertion into the arylic C–H bond in substrates having substituents at the nitrogen atom with primary, secondary, as well as tertiary Csp$^3$–H bonds. Notably, ((IMes)Pd(NQ))$_2$ was more efficient than Pd$_2$(dba)$_3$ in promoting the insertion of *N*-alkylacetanilides lacking substituents on the arylic ring (**1b**–**1d**) (Table 2, entries 1–6) or bearing an electron-donating substituent (**1g**) (Table 2, entries 11–12). In contrast, the introduction of electron-withdrawing groups dramatically diminished the catalytic efficiency of ((IMes)Pd(NQ))$_2$. Thus, for example, acetanilide **1f**, bearing an *ortho*-bromo substituent, was recovered unchanged when using ((IMes)Pd(NQ))$_2$, whereas in the presence of Pd$_2$(dba)$_3$, it afforded oxindole **2f** in 23% yield (Table 2, entries 9 and 10). Oxindole **2h**, with a fluoro group, was isolated in a modest 39% yield when using ((IMes)Pd(NQ))$_2$ but obtained in an acceptable 64% yield in the presence of Pd$_2$(dba)$_3$ (Table 2, entries 13–14). No insertion product was formed in the ((IMes)Pd(NQ))$_2$-catalyzed reaction of acetanilide **1i**, which bears a methoxycarbonyl substituent, while oxindole **2i** was isolated in 22% yield when using Pd$_2$(dba)$_3$ (Table 2, entries 15–16). ((IMes)Pd(NQ))$_2$ also gave worse results in the sequential insertion/alkylation sequence from *N,N*-diphenylacetamide **1e** (Table 2, entries 7 and 8) and *N*-naphthylacetamide **1j** (Table 2, entries 17–18).

At this point, we studied the decomposition of α-diazo-*N*-pyridinylacetamide **3**, which, upon treatment with a catalytic amount of ((IMes)Pd(NQ))$_2$ under the optimized reaction conditions, afforded mesoionic compound **4** (77%), resulting from the interception of the transient metallacarbene by the pyridine nitrogen (Scheme 4). This kind of mesoionic imidazopyridines have been previously prepared [61] and show interesting insecticidal activity [62].
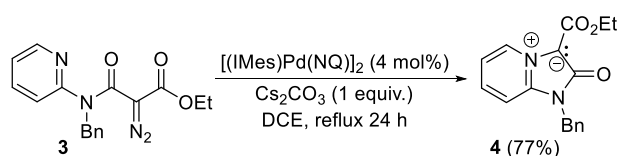


**Scheme 4.** Pd-catalyzed cyclization of α-diazoamide **3**.

Regarding the palladium-catalyzed reactions shown in Tables 1 and 2, it should be noted that the formation of β-lactam products, resulting from the possible competitive carbene Csp$^3$–H insertion, was not observed. This sharply contrasts with the competition between the carbene C$_{Ar}$sp$^2$–H and Csp$^3$–H insertions observed in Rh(II)-promoted processes (see, for instance, Scheme 1(a)) [48].

Our previously reported DFT calculations suggested that the Pd(0)-catalyzed C$_{Ar}$sp$^2$–H insertion of α-diazo-α-(methoxycarbonyl)acetanilides to give oxindoles proceeds via a genuine stepwise mechanism involving a Pd-mediated 1,5-hydrogen migration from the initially generated pallada(0)carbene complex, followed by a reductive elimination [55]. It was also shown that the complete chemoselectivity of the process, which exclusively produces oxindoles over β-lactams, takes place mainly under kinetic control. We now decided to check the generality of this unprecedented Pd(0)-mediated mechanism using the model Pd(NHC) (NHC = 1,3-bis(phenyl)-imidazil-2-ylidene) catalyst.

Figure 1 shows the computed reaction profile for the formation of oxindole **2b'**, precursor of the experimentally observed oxindole **2b** (see Table 2). As expected, based on our previous report [55], the process begins from pallada(0)carbene **INT0**, formed upon reaction of α-diazoamide **1b** and the active catalyst species Pd(NHC). This species evolves into intermediate **INT1** in a highly exergonic process ($\Delta G_R$ = −25.3 kcal/mol) through the transition state **TS1** with a computed activation barrier of 16.2 kcal/mol, which is fully compatible with the reaction conditions used in the experiment. Closer inspection of **TS1** indicates that this reaction step can be viewed as a Pd-mediated 1,5-hydrogen migration, which involves the formal oxidation of the transition metal. The alternative Csp$^3$–H activation reaction via **TS1'**, which would involve an analogous Pd-mediated 1,4-hydrogen migration, is not competitive in view of the much higher activation barrier ($\Delta G^{\neq}$ = 8.2 kcal/mol) computed for this alternative transformation. Therefore, it is once again found that the complete selectivity of the process takes place under kinetic control. The transformation ends with an exergonic ($\Delta G_R$ = −6.8 kcal/mol)

reductive elimination reaction that directly transforms **INT1** into oxindole **2b'** with the concomitant release of the active catalytic species Pd(NHC) through the transition state **TS2** (with a feasible activation barrier of 18.7 kcal/mol).
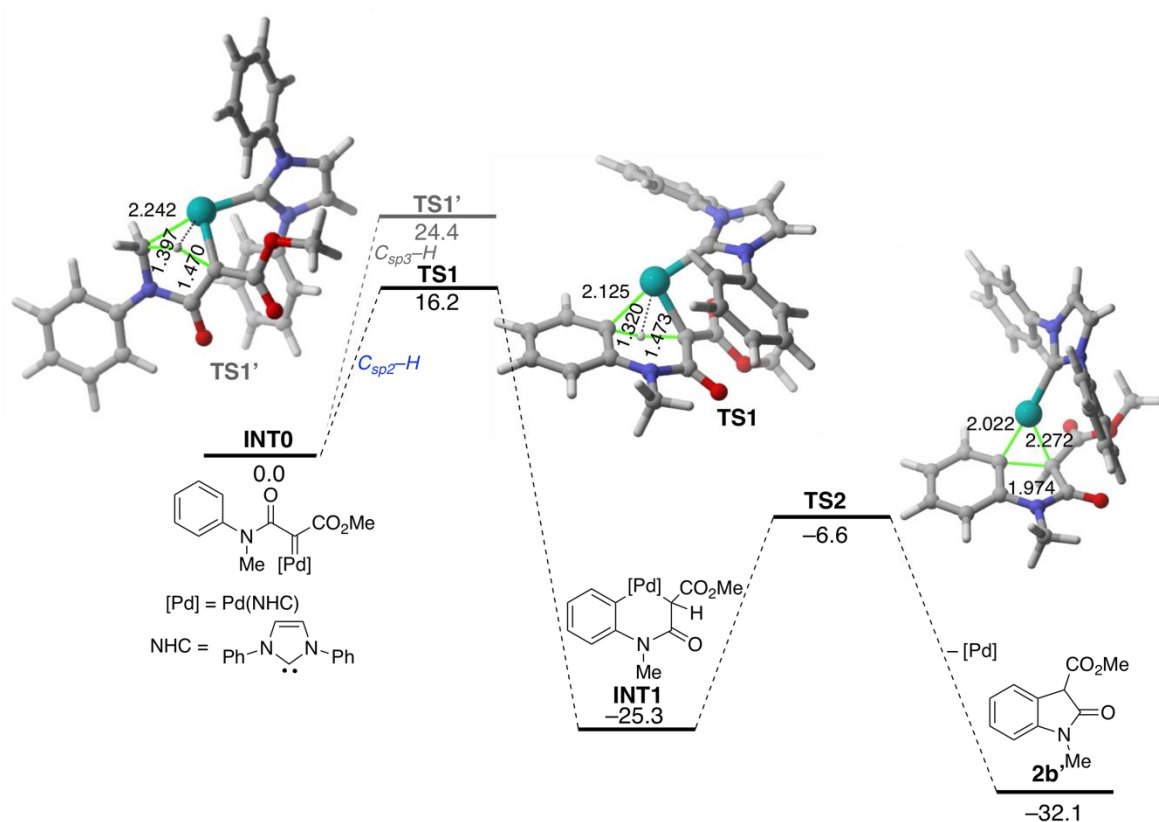


**Figure 1.** Computed reaction profile for the transformation of pallada(0)carbene **INT0** into oxindole **2b'**: Relative free energies and bond distances are given in kcal/mol and angstroms, respectively. All data have been computed at the PCM(dichloroethane)-B3LYP-D3/def2-TZVPP//PCM(dichloroethane)-B3LYP-D3/def2-SVP level.

On the other hand, we have also reported that the intramolecular carbene C–H insertion of α-diazo-α-(methoxycarbonyl)acetamides to form β-lactams can be effectively catalyzed by Pd(II) complexes (Scheme 2b) [56]. Due to its ubiquitous presence in the molecular structure of natural products and biologically active compounds, β-lactam synthesis has attracted considerable attention over the years [63–65]. To further understand the impact of the electronic nature of the catalyst in the aforementioned insertion reaction, we decided to explore the use of some Pd(0)-precatalysts. Table 3 shows the results of the reactions of diversely substituted *N*-benzyl-*N*-*t*butyl-α-diazoacetamides (**5a–5m**) when using either Pd$_2$(dba)$_3$ or ((IMes)Pd(NQ))$_2$ as the catalyst and compares them with those previously obtained in the Pd(II)-catalyzed reactions [56].

**Table 3.** Palladium-catalyzed cyclization reactions of $\alpha$-diazoamides **5a–5m** [1].
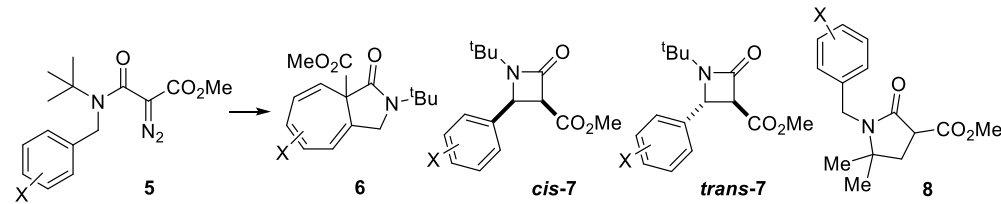
| Entry | 5 (X) | Catalyst (mol%) | 6/7/8 [2,3] | cis-7/trans-7 [2,3] | Products (Yield (%)) [4] |
|---|---|---|---|---|---|
| 1 | **5a** (H) | Pd$_2$(dba)$_3$ (10) | 26/74/0 | 46/28 | **6a** (20) / *cis*-**7a** (9), *trans*-**7a** (42) |
| 2 | **5a** (H) | ((IMes)Pd(NQ))$_2$ (2.5) | 35/65/0 | 40/25 | **6a** (28) / *cis*-**7a** (35), *trans*-**7a** (23) |
| 3 | **5a** (H) | (Pd(allyl)Cl)$_2$ (5) | 0/100/0 | 47/53 | *cis*-**7a** (25), *trans*-**7a** (65) |
| 4 | **5a** (H) | (SIPr)Pd(allyl)Cl (15) | 0/100/0 | 29/71 | *cis*-**7a** (17), *trans*-**7a** (59) |
| 5 | **5b** (4-MeO) | Pd$_2$(dba)$_3$ (10) | 50/50/0 | 21/29 | **6b** (24) / *cis*-**7b** (9), *trans*-**7b** (20) |
| 6 | **5b** (4-MeO) | ((IMes)Pd(NQ))$_2$ (2.5) | 34/66/0 | 46/20 | **6b** (22) / *cis*-**7b** (21), *trans*-**7b** (24) |
| 7 | **5b** (4-MeO) | (Pd(allyl)Cl)$_2$ (5) | 14/86/0 | 29/57 | **6b** (8) / *cis*-**7b** (18), *trans*-**7b** (39) |
| 8 | **5b** (4-MeO) | (SIPr)Pd(allyl)Cl (15) | 16/84/0 | 42/42 | **6b** (10) / *cis*-**7b** (8), *trans*-**7b** (52) |
| 9 | **5c** (4-MeS) | Pd$_2$(dba)$_3$ (10) | 18/82/0 | 36/46 | **6c** (6) / *cis*-**7c** (4), *trans*-**7c** (30) |
| 10 | **5c** (4-MeS) | ((IMes)Pd(NQ))$_2$ (2.5) | 11/89/0 | 68/21 | **6c** (7) / *cis*-**7c** (30), *trans*-**7c** (50) |
| 11 | **5c** (4-MeS) | (Pd(allyl)Cl)$_2$ (5) | 5/95/0 | 42/53 | *cis*-**7c** (10), *trans*-**7c** (48) |
| 12 | **5c** (4-MeS) | (SIPr)Pd(allyl)Cl (15) | 12/88/0 | 48/40 | **6c** (7) / *cis*-**7c** (4), *trans*-**7c** (60) |
| 13 | **5d** (4-Cl) | Pd$_2$(dba)$_3$ (10) | 15/85/0 | 8/77 | **6d** (9) / *cis*-**7d** (5), *trans*-**7d** (50) |
| 14 | **5d** (4-Cl) | ((IMes)Pd(NQ))$_2$ (2.5) | 5/95/0 | 69/26 | **6d** (5) / *cis*-**7d** (53), *trans*-**7d** (19) |
| 15 | **5d** (4-Cl) | (Pd(allyl)Cl)$_2$ (5) | 0/100/0 | 52/48 | *cis*-**7d** (42), *trans*-**7d** (40) |
| 16 | **5d** (4-Cl) | (SIPr)Pd(allyl)Cl (15) | 0/100/0 | 62/38 | *cis*-**7d** (27), *trans*-**7d** (42) |
| 17 | **5e** (4-CN) | Pd$_2$(dba)$_3$ (10) | 3/97/0 | 67/30 | *cis*-**7e** (22), *trans*-**7e** (38) |
| 18 | **5e** (4-CN) | ((IMes)Pd(NQ))$_2$ (2.5) | 5/75/20 | 25/50 | *cis*-**7e** (15), *trans*-**7e** (33) / **8e** (15) |
| 19 | **5e** (4-CN) | (Pd(allyl)Cl)$_2$ (5) | 0/100/0 | 71/29 | *cis*-**7e** (34), *trans*-**7e** (36) |
| 20 | **5e** (4-CN) | (SIPr)Pd(allyl)Cl (15) | 0/100/0 | 38/62 | *cis*-**7e** (27), *trans*-**7e** (51) |
| 21 | **5f** (4-NMe$_2$) | Pd$_2$(dba)$_3$ (10) | CM | — | — |
| 22 | **5f** (4-NMe$_2$) | ((IMes)Pd(NQ))$_2$ (2.5) | CM | — | *cis*-**7f** (9), *trans*-**7f** (10) / **10** (15) [5] |
| 23 | **5f** (4-NMe$_2$) | (Pd(allyl)Cl)$_2$ (5) | CM | — | *trans*-**7f** (14), **10** (36) |
| 24 | **5f** (4-NMe$_2$) | (SIPr)Pd(allyl)Cl (15) | CM | — | *trans*-**7f** (10), **10** (45) |
| 25 | **5g** (3-Cl) | Pd$_2$(dba)$_3$ (10) | 8/92/0 | 54/38 | **6g** [6] (7) / *cis*-**7g** (30), *trans*-**7g** (43) |
| 26 | **5g** (3-Cl) | ((IMes)Pd(NQ))$_2$ (2.5) | 6/94/0 | 73/21 | **6g** [6] (5) / *cis*-**7g** (50), *trans*-**7g** (20) |
| 27 | **5g** (3-Cl) | (Pd(allyl)Cl)$_2$ (5) | 0/100/0 | 64/36 | *cis*-**7g** (44), *trans*-**7g** (36) |
| 28 | **5g** (3-Cl) | (SIPr)Pd(allyl)Cl (15) | 0/100/0 | 50/50 | *cis*-**7g** (30), *trans*-**7g** (31) |
| 29 | **5h** (3-CN) | Pd$_2$(dba)$_3$ (10) | 0/100/0 | 33/67 | *cis*-7h (25), *trans*-7h (48) |
| 30 | **5h** (3-CN) | ((IMes)Pd(NQ))$_2$ (2.5) | 4/74/22 | 30/44 | *cis*-**7h** (15), *trans*-7h (37) / **8h** (6) |
| 31 | **5h** (3-CN) | (Pd(allyl)Cl)$_2$ (5) | 0/100/0 | 47/53 | *cis*-**7h** (22), *trans*-7h (43) |
| 32 | **5h** (3-CN) | (SIPr)Pd(allyl)Cl (15) | 0/100/0 | 29/71 | *cis*-**7h** (15), *trans*-**7h** (55) |
| 33 | **5i** (2-MeO) | Pd$_2$(dba)$_3$ (10) | 14/86/0 | 43/43 | **6i** (8) / *cis*-**7i** (12), *trans*-**7i** (19) |

**Table 3.** *Cont.*



| Entry | 5 (X) | Catalyst (mol%) | 6/7/8 [2,3] | cis-7/trans-7 [2,3] | Products (Yield (%)) [4] |
|---|---|---|---|---|---|
| 34 | **5i** (2-MeO) | ((IMes)Pd(NQ))₂ (2.5) | 20/80/0 | 57/23 | **6i** (10)<br>cis-**7i** (45), trans-**7i** (24) |
| 35 | **5i** (2-MeO) | (Pd(allyl)Cl)₂ (5) | 5/95/0 | 42/53 | cis-**7i** (23), trans-**7i** (31) |
| 36 | **5i** (2-MeO) | (SIPr)Pd(allyl)Cl (15) | 6/94/0 | 39/55 | cis-**7i** (10), trans-**7i** (63) |
| 37 | **5j** (2-F) | Pd₂(dba)₃ (10) | 8/92/0 | 8/84 | cis-**7j** (5), trans-**7j** (66) |
| 38 | **5j** (2-F) | ((IMes)Pd(NQ))₂ (2.5) | 5/83/12 | 24/59 | cis-**7j** (10), trans-**7j** (62)<br>**8j** (11) |
| 39 | **5j** (2-F) | (Pd(allyl)Cl)₂ (5) | 0/100/0 | 69/31 | cis-**7j** (26), trans-**7j** (56) |
| 40 | **5j** (2-F) | (SIPr)Pd(allyl)Cl (15) | 0/100/0 | 0/100 | trans-**7j** (66) |
| 41 | **5k** (2-Br) | Pd₂(dba)₃ (10) | 7/93/0 | 70/23 | **6k** (6)<br>cis-7k (46), trans-**7k** (15) |
| 42 | **5k** (2-Br) | ((IMes)Pd(NQ))₂ (2.5) | 0/85/15 | 66/19 | cis-**7k** (43), trans-**7k** (20)<br>**8k** (12) |
| 43 | **5k** (2-Br) | (Pd(allyl)Cl)₂ (5) | 14/86/0 | 52/34 | **6k** (9)<br>cis-**7k** (34), trans-**7k** (31) |
| 44 | **5k** (2-Br) | (SIPr)Pd(allyl)Cl (15) | 8/92/0 | 21/71 | **6k** (4)<br>cis-7k (8), trans-**7k** (42) |
| 45 | **5l** (2-I) | Pd₂(dba)₃ (10) | 0/100/0 | 9/91 | cis-**7l** (5), trans-**7l** (45) |
| 46 | **5l** (2-I) | ((IMes)Pd(NQ))₂ (2.5) | 0/78/22 | 66/12 | cis-**7l** (64), trans-**7l** (12)<br>**8l** (15) |
| 47 | **5l** (2-I) | (Pd(allyl)Cl)₂ (5) | 8/92/0 | 50/42 | **6l** (9)<br>cis-**7l** (49), trans-**7l** (38) |
| 48 | **5l** (2-I) | (SIPr)Pd(allyl)Cl (15) | 0/100/0 | 77/23 | cis-**7l** (53), trans-**7l** (15) |
| 49 | **5m** (3-MeO, 4-MeO) | Pd₂(dba)₃ (10) | 50/50/0 | 21/29 | **6m** (25)<br>cis-**7m** (11), trans-**7m** (20) |
| 50 | **5m** (3-MeO, 4-MeO) | ((IMes)Pd(NQ))₂ (2.5) | 32/68/0 | 44/24 | **6m** (13)<br>cis-**7m** (23), trans-**7m** (30) |
| 51 | **5m** (3-MeO, 4-MeO) | (Pd(allyl)Cl)₂ (5) | 15/85/0 | 8/77 | **6m** (6)<br>trans-**7m** (39) |
| 52 | **5m** (3-MeO, 4-MeO) | (SIPr)Pd(allyl)Cl (15) | 24/76/0 | 43/33 | **6m** (9)<br>cis-**7m** (6), trans-**7m** (38) |

[1] Reaction conditions: Catalyst (see table) in DCE at reflux for 24 h. [2] Ratios determined by integration of characteristic ¹H-NMR absorptions from the spectrum of the reaction mixture. [3] The majority of reactions were performed twice, while the Buchner:β-lactam:γ-lactam ratio (**6/7/8**) was essentially the same in the two runs and the *cis:trans* ratio was quite different due to the partial isomerization of *cis* β-lactams to the more stable *trans* isomers during the work-up or even when recording the ¹H-NMR spectra. [4] Yields refer to products isolated by chromatography. [5] 4-(Dimethylamino)benzaldehyde (**10**). [6] Mixture of regioisomers.

The examples in Table 3 confirm the generality and functional group tolerance of Pd₂(dba)₃ and ((IMes)Pd(NQ))₂ as catalysts for these insertion processes. Although both Pd(0) and Pd(II) catalysts can be used to promote $Csp^3$–H insertion, some significant differences were identified. On the whole, the Pd(II) complexes proved to be more versatile for β-lactam formation despite not always giving the highest yield. In general, the resulting β-lactams were obtained in moderate to good overall yields (53–90%), usually as mixtures of *cis* and *trans* isomers, in transformations proceeding with high site selectivity, except when using **5f**. In this particular case, the use of Pd(II) catalysts to promote its decomposition resulted in the formation of *trans*-**7f** (10–14%), together with major amounts of aldehyde **10**. On the other hand, when ((IMes)Pd(NQ))₂ was used, a complex reaction mixture was obtained, from which *cis*-**7f** (9%), *trans*-**7f** (10%), and aldehyde **10** (15%) were isolated, while no cyclization product was obtained in the presence of Pd₂(dba)₃.

Notably, partial or complete isomerization of the *cis* β-lactam to the more stable *trans* isomer took place during the chromatographic purification of the reaction mixtures, which explains the observed differences in *cis/trans* ratios before and after purification.

The effect of adding phosphine ligands to the Pd(0) catalyst was also explored. However, similarly to the oxindole-forming reactions, the use of Pd$_2$(dba)$_3$ in the presence of phosphine ligands resulted in slower reaction rates. Thus, for example, treatment of **5a** with Pd$_2$(dba)$_3$ (10 mol%) in the presence of (*o*-tolyl)$_3$P (20 mol%) under otherwise the same reaction conditions gave a mixture of **6** (12%), *cis*-**7** (22%), and *trans*-**7** (26%) together with some unreacted α-diazoamide (10%) (result not included in the table).

Interestingly, no product from the potentially competitive palladium-catalyzed cross-coupling of the aryl halide with the α-diazoamide moiety [32–35] was observed in the reactions of **5k** (Table 3, entries 41–42) and **5l** (Table 3, entries 45–46) when using Pd(0) catalysts.

As can be seen in Table 3, the effect of the substituent at the benzyl group on the outcome of the process varied according to its electronic nature as well as its position on the aromatic ring. The introduction of electron-donor groups led to an increased formation of the cycloheptapyrrolone product, especially when using Pd(0) catalysts. The increase was lower when the substituent was located at the *ortho*-position, probably due to steric interactions. In contrast, the electron-withdrawing groups generally diverted the palladacarbene away from the Buchner reaction in favor of the Csp$^3$–H insertion. Similar electronic effects have been observed in related Rh(II)-catalyzed transformations [48]. On the other hand, the use of ((IMes)Pd(NQ))$_2$ as the catalyst in the reaction of those substrates bearing electron-withdrawing groups resulted in the formation of minor amounts of the corresponding γ-lactam (**8**), which arises from the *t*butyl Csp$^3$–H insertion. Notably, the γ-lactams were not observed when using Pd(II) catalysts.

The above results also confirm the significant impact of the electronic nature of the Pd catalyst and ensue electrophilicity of the carbene intermediate in the reaction pathway. Thus, whereas benzylic Csp$^3$–H insertion is strongly favored over the Buchner reaction when using Pd(II), an increased cycloheptapyrrolone product formation is usually observed with the more electron-rich Pd(0) complexes. Interestingly, Rh(II)-catalyzed transformations show opposite reactivity trends, in which highly electrophilic Rh(II) complexes favor Buchner reactions over benzylic Csp$^3$–H insertion [44–46].

Finally, we explored the transition metal-catalyzed decomposition of α-diazoacetamide **11**, which bears a (4-pyridinyl)methyl group instead of the *N*-benzyl substituent (Table 4). Treatment of **11** with a catalytic amount of ((IMes)Pd(NQ))$_2$ under the optimized reaction conditions resulted in the complete decomposition of the material (Table 4, entry 1). When the reaction was performed at lower temperatures (refluxing dichloromethane), **11** was recovered unchanged (Table 4, entry 2). In contrast, the use of Pd(II) catalysts (Table 4, entries 3 and 4) resulted in the formation of β-lactam **12** (*cis/trans* mixture), with (SIPr)Pd(allyl)Cl affording the highest yield. Interestingly, α-diazoacetamide **11** was recovered unchanged when using the well-known (Rh(OAc)$_2$)$_2$ catalyst (Table 4, entry 5).

**Table 4.** Transition metal-catalyzed reactions of α-diazoamide **11** [1].



| Entry | Catalyst (mol%) | Solvent | Temp. | Time | Products (Yield (%)) [2] |
|---|---|---|---|---|---|
| 1 | ((IMes)Pd(NQ))$_2$ (2.5) | DCE | reflux | 24 h | — |
| 2 | ((IMes)Pd(NQ))$_2$ (2.5) | CH$_2$Cl$_2$ | reflux | 24 h | **11** |
| 3 | (Pd(allyl)Cl)$_2$ (5) | DCE | reflux | 24 h | *cis*-**12**/*trans*-**12** (1:10, 30%) |
| 4 | (SIPr)Pd(allyl)Cl (15) | DCE | reflux | 48 h | *cis*-**12**/*trans*-**12** (1:2.2, 54%) |
| 5 | (Rh(OAc)$_2$)$_2$ (3) | CH$_2$Cl$_2$ | r.t. | 24 h | **11** |

[1] All reactions were conducted with **11** (0.2 mmol). [2] Isolated yield.

In our previous work on the synthesis of β-lactams, we studied computationally the Pd(II)-catalyzed insertion reaction of α-diazo-α-(methoxycarbonyl)acetamides [56]. According to our DFT calculations, this insertion reaction also occurs stepwise and involves an unprecedented Pd(II)-promoted Mannich-type reaction through a pallada(II)carbene-induced zwitterionic intermediate. To shed light on the reaction mechanism and the influence of the Pd(0) catalyst on the selectivity of the C–H insertion described above, DFT calculations were also carried out. To this end, the process involving **5a** in the presence of the model Pd(NHC) (NHC = 1,3-bis(phenyl)-imidazil-2-ylidene) catalyst was explored.

Figure 2 shows the computed reaction profile for the transformation of the initially formed pallada(0)carbene intermediate **INT0** into the observed β-lactams *cis-***7a** and *trans-***7a**. Similar to the reaction profile computed for the formation of oxindoles discussed above (Figure 1), the initial **INT0** readily evolves into the corresponding five-membered pallada(II)cycle **INT1** via the transition state **TS1** in a highly exergonic transformation ($\Delta G_R \approx -40$ kcal/mol). Once again, this saddle point is associated with a 1,4-hydrogen migration reaction mediated by the transition metal fragment, thus confirming the generality of this type of C–H insertion reaction. Then, species **INT1** is transformed into the final β–lactam through a reductive elimination reaction via **TS2**, which releases the active catalyst able to enter into a new catalytic cycle. Interestingly, the computed *cis/trans* activation barrier differences for either the initial 1,4-H migration ($\Delta G^{\neq} = 1.3$ kcal/mol) or for the subsequent elimination reaction ($\Delta G^{\neq} = 0.2$ kcal/mol) indicates that the formation of the *cis-***7a** β-lactam should be only slightly favored over the formation of its *trans* counterpart, which nicely matches the experimental findings (see Table 3, entry 2).
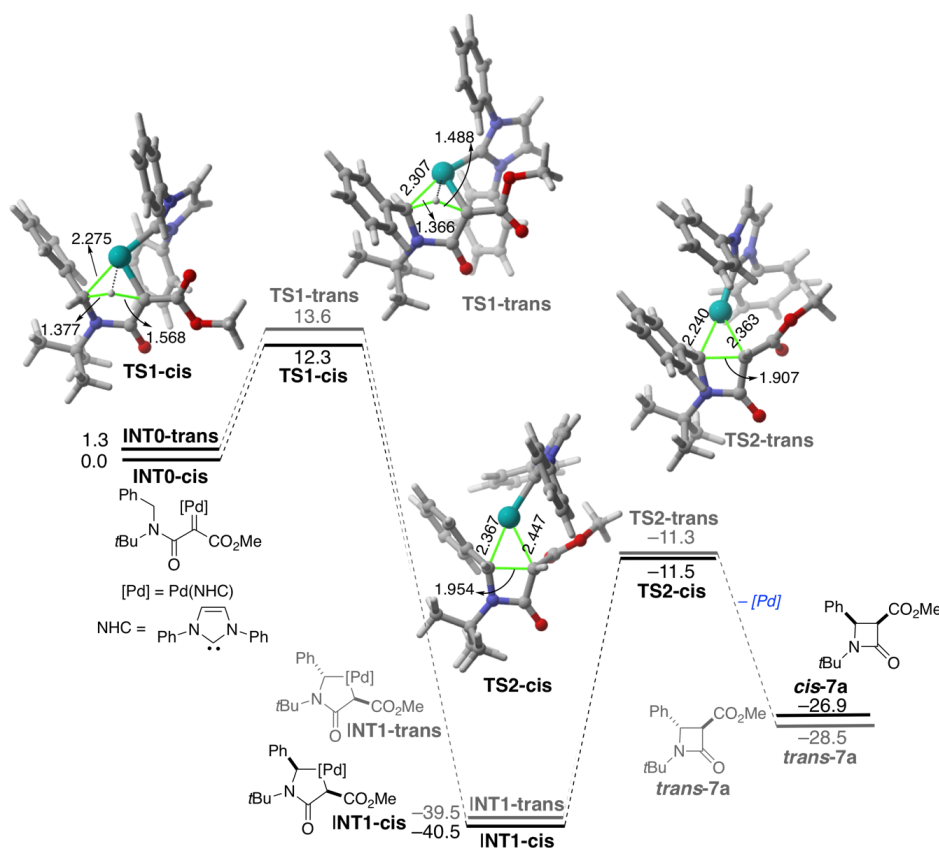


**Figure 2.** Computed reaction profile for the transformation of pallada(0)carbene **INT0** into β-lactams *cis-***7a** and *trans-***7a**: Relative free energies and bond distances are given in kcal/mol and angstroms, respectively. All data have been computed at the PCM(dichloroethane)-B3LYP-D3/def2-TZVPP//PCM(dichloroethane)-B3LYP-D3/def2-SVP level.

## 3. Materials and Methods

### 3.1. General Information

All commercially available reagents were used without further purification. $^1$H- and $^{13}$C-NMR spectra were recorded using Me$_4$Si as the internal standard with a Varian Mercury 400 instrument (Oxford, United Kingdom). Chemical shifts are reported in ppm downfield ($\delta$) from Me$_4$Si for $^1$H and $^{13}$C-NMR. TLC was carried out on SiO$_2$ (silica gel 60 F$_{254}$, Merck), and the spots were located with UV light or 1% aqueous KMnO$_4$. Flash chromatography was carried out on SiO$_2$ (silica gel 60, SDS, 230–400 mesh ASTM). Organic extracts were dried over anhydrous Na$_2$SO$_4$ during workup of reactions. Evaporation of solvents was accomplished with a rotatory evaporator (Büchi, Flavill, Switzerland). $\alpha$-Diazoacetamides **1a**–**1j** and oxindoles **2a**–**2j** are known compounds previously prepared by us [55], as are $\alpha$-diazoacetamides **5a**–**5m** and $\beta$-lactams **7a**–**7m** [56].

### 3.2. Synthesis of N-Benzyl-N-(2-pyridinyl)-α-(ethoxycarbonyl)-α-diazoacetamide (**3**).

To a solution of 2-benzylaminopyridine (0.5 g, 2.71 mmol) and Et$_3$N (0.39 mL, 2.71 mmol) in CH$_2$Cl$_2$ (10 mL), cooled at 0 °C, ethyl malonyl chloride (0.38 mL, 2.71 mmol) was added slowly. The mixture was stirred at room temperature for 24 h. After the reaction was completed, the mixture was poured into water and extracted with CH$_2$Cl$_2$. The organic extracts were washed with saturated NaHCO$_3$ aqueous solution, dried, filtered, and concentrated. The residue was purified by chromatography (SiO$_2$, from CH$_2$Cl$_2$ to CH$_2$Cl$_2$/MeOH 97:3) to give *N*-benzyl-*N*-(2-pyridinyl)-$\alpha$-(ethoxycarbonyl) acetamide (0.77 g, 95%).

To a solution of *N*-benzyl-*N*-(2-pyridinyl)-$\alpha$-(ethoxycarbonyl)acetamide (0.25 g, 0.84 mmol) and Et$_3$N (0.14 mL, 1.0 mmol) in dry acetonitrile (15 mL), *p*-toluenesulfonylazide (2.6 mL of a 11% solution in toluene, 1.45 mmol) was added dropwise. The mixture was stirred at room temperature for 90 h. The solvent was removed in vacuo, and the resulting residue was partitioned between CH$_2$Cl$_2$ and 10% NaOH aqueous solution. The organic extracts were dried, filtered, and concentrated. The residue was purified by chromatography (SiO$_2$, from CH$_2$Cl$_2$ to CH$_2$Cl$_2$/MeOH 99:1) to give *N*-benzyl-*N*-(2-pyridinyl)-$\alpha$-(ethoxycarbonyl)-$\alpha$-diazoacetamide (**3**, 150 mg; 55%) as a brown oil. $^1$H-NMR (CDCl$_3$, 400 MHz) $\delta$ 1.07 (t, *J* = 7.2 Hz, 3H), 3.92 (q, *J* = 7.2 Hz, 2H), 5.22 (s, 2H), 7.04 (ddd, *J* = 7.4, 4.8, and 0.8 Hz, 1H), 7.10 (dt, *J* = 8.4 and 0.8 Hz, 1H), 7.20 (tt, *J* = 7.2 and 1.2 Hz, 1H), 7.23–7.29 (m, 2H), 7.32–7.36 (m, 2H), 7.60 (ddd, *J* = 8.4, 7.4 and 2.0 Hz, 1H), and 8.40 (ddd, *J* = 4.8, 2.0 and 0.8 Hz, 1H). $^{13}$C-NMR (CDCl$_3$, 100.6 MHz) $\delta$ 14.3 (CH$_3$), 52.3 (CH$_2$), 61.4 (CH$_2$), 70.2 (C), 118.3 (CH), 120.8 (CH), 127.4 (CH), 127.9 (2 CH), 128.6 (2 CH), 137.5 (C), 138.0 (CH), 148.6 (CH), 156.1 (C), 161.4 (C), and 162.3 (C).

### 3.3. Synthesis of N-tert-Butyl-N-(4-pyridinylmethyl)-α-(methoxycarbonyl)-α-diazoacetamide (**11**).

To a solution of *N*-tert-butyl-*N*-(4-pyridinylmethyl)amine (0.67 g, 4.1 mmol) and Et$_3$N (0.58 mL, 4.1 mmol) in CH$_2$Cl$_2$ (20 mL), cooled at 0 °C, methyl malonyl chloride (0.57 mL, 5.3 mmol) was added slowly. The mixture was stirred at room temperature for 24 h. After the reaction was completed, the mixture was poured into water and extracted with CH$_2$Cl$_2$. The organic extracts were washed with saturated NaHCO$_3$ aqueous solution, dried, filtered, and concentrated to give *N*-tert-butyl-*N*-(4-pyridinylmethyl)-$\alpha$-(methoxycarbonyl)acetamide as an orange oil (0.98 g, 90%), which was used in the next reaction without purification.

To a solution of *N*-tert-butyl-*N*-(4-pyridinylmethyl)-$\alpha$-(methoxycarbonyl)acetamide (0.5 g, 1.89 mmol) and DBU (0.45 mL, 2.85 mmol) in dry acetonitrile (6 mL), a solution of p-ABSA (515 mg, 2.1 mmol) in dry acetonitrile (2 mL) was added dropwise. The mixture was stirred at room temperature overnight. The solvent was removed in vacuo, and the resulting residue was partitioned between CH$_2$Cl$_2$ and 10% NaOH aqueous solution. The organic extracts were dried, filtered, and concentrated. The residue was purified by chromatography (SiO$_2$, from CH$_2$Cl$_2$ to CH$_2$Cl$_2$/MeOH 98:2) to give *N*-tert-butyl-*N*-(4-pyridinylmethyl)-$\alpha$-(methoxycarbonyl)-$\alpha$-diazoacetamide (**11**, 145 mg; 26%) as an

orange oil. ^{1}H-NMR (CDCl$_3$, 400 MHz) δ 1.40 (s, 9H), 3.77 (s, 3H), 4.63 (s, 2H), 7.15 (d, *J* = 6.0 Hz, 2H), and 7.57 (d, *J* = 6.0 Hz, 2H). ^{13}C-NMR (CDCl$_3$, 100.6 MHz) δ 29.0 (3 CH$_3$), 50.6 (CH$_2$), 52.4 (CH$_3$), 59.5 (C), 68.7 (C), 121.9 (2 CH), 149.3 (C), 150.2 (2 CH), 162.8 (C), and 163.5 (C).

*3.4. Characterization Data for New Compounds of Scheme 4 and Tables 3 and 4*

*1-Benzyl-3-(ethoxycarbonyl)-2-oxo-2,3-dihydro-1H-imidazo (1,2-a)pyridin-4-ium-3-ylide* (**4**). Amorphous orange solid. ^{1}H-NMR (CDCl$_3$, 400 MHz) δ 1.45(t, *J* = 7.2 Hz, 3H), 4.43 (q, *J* = 7.2 Hz, 2H), 5.20 (s, 2H), 6.99 (ddd, *J* = 8.8, 1.6, and 0.8 Hz, 1H), 7.08 (ddd, *J* = 7.6, 6.8, and 1.2 Hz, 1H), 7.25–7.37 (m, 5H), 7.40 (ddd, *J* = 8.8, 7.6, and 1.2 Hz, 1H), 9.65 (d, *J* = 6.8 Hz, 1H). ^{13}C-NMR (CDCl$_3$, 100.6 MHz) δ 14.9 (CH$_3$), 43.3 (CH$_2$), 60.0 (CH$_2$), 94.0 (C), 106.4 (CH), 115.7 (CH), 127.8 (2 CH), 128.2 (CH), 129.0 (CH), 129.1 (2 CH), 129.9 (CH), 135.4 (C), 135.6 (C), 157.0 (C), and 162.6 (C).

*Methyl 2-tert-butyl-6-chloro-3-oxo-1H-2,3-dihydrocyclohepta(c)pyrrole-3a-carboxylate* (**6d**). ^{1}H-NMR (CDCl$_3$, 400 MHz, signals from a 4.5:1 mixture of **trans-7d** and **6d**) δ 1.45 (s, 9H), 3.64 (s, 3H), 4.21 (dd, *J* = 14.8 and 1.2 Hz, 1H), 4.44 (d, *J* = 14.8 Hz, 1H), 5.63 (d, *J* = 10.2 Hz, 1H), 6.17 (d, *J* = 6.8 Hz, 1H), 6.39 (d, *J* = 10.2 Hz, 1H), and 6.62 (d, *J* = 6.8 Hz, 1H).

*Methyl 1-(4-cyanobenzyl)-5,5-dimethyl-2-oxopyrrolidine-3-carboxylate* (**8e**). Amorphous orange solid. ^{1}H-NMR (CDCl$_3$, 400 MHz) δ 1.16 (s, 3H), 1.22 (s, 3H), 2.19 (dd, *J* = 13.2 and 9.2 Hz, 1H), 2.33 (dd, *J* = 13.2 and 9.2 Hz, 1H), 3.62 (t, *J* = 9.2 Hz, 1H), 3.82 (s, 3H), 4.33 (d, *J* = 16.0 Hz, 1H), 4.60 (d, *J* = 16.0 Hz, 1H), 7.39 (d, *J* = 8.4 Hz, 2H), 7.60 (d, *J* = 8.4 Hz, 2H). ^{13}C-NMR (CDCl$_3$, 100.6 MHz) δ 27.1 (CH$_3$), 28.1 (s, CH$_3$), 38.3 (CH$_2$), 43.2 (CH$_2$), 47.4 (CH), 53.0 (CH$_3$), 60.0 (C), 111.5 (C), 118.8 (C), 128.3 (2 CH), 132.6 (2 CH), 143.9 (C), 170.2 (C), and 170.9 (C).

*Methyl cis-1-tert-butyl-4-[4-(dimethylamino)phenyl]-2-oxoazetidine-3-carboxylate* (cis-**7f**). Amorphous orange solid. ^{1}H-NMR (CDCl$_3$, 400 MHz) δ 1.30 (s, 9H), 2.95 (s, 6H), 3.40 (s, 3H), 4.18 (d, *J* = 6.0 Hz, 1H), 4.83 (d, *J* = 6.0 Hz, 1H), 6.65 (d, *J* = 8.8 Hz, 2H), and 7.21 (d, *J* = 8.8 Hz, 2H).

*Methyl 2-tert-butyl-7-chloro-3-oxo-1H-2,3-dihydrocyclohepta[c]pyrrole-3a-carboxylate (6g)*. ^{1}H-NMR (CDCl$_3$, 400 MHz, signals from a 11:1 mixture of *trans-***7g** and **6g**) δ 1.45 (s, 9H), 3.64 (s, 3H), 4.22 (dd, *J* = 15.6 and 2.0 Hz, 1H), 4.47 (dd, *J* = 15.6 and 2.4 Hz, 1H), 5.60 (d, *J* = 9.6 Hz, 1H), 6.27–6.30 (m, 1H), 6.32 (dd, *J* = 9.6 and 7.2 Hz, 1H), and 6.61 (dd, *J* = 7.2 and 1.2 Hz, 1H).

*Methyl 2-tert-butyl-5-chloro-3-oxo-1H-2,3-dihydrocyclohepta[c]pyrrole-3a-carboxylate (6g')*. ^{1}H-NMR (CDCl$_3$, 400 MHz, signals from a 12:4:1 mixture of *trans-***7g**, **6g**, and **6g'**) δ 1.46 (s, 9H), 3.64 (s, 3H), 4.23 (dd, *J* = 15.2 and 2.0 Hz, 1H), 4.42 (dd, *J* = 15.2 and 2.4 Hz, 1H), 5.76 (t, *J* = 1.2 Hz, 1H), 6.18–6.21 (m, 1H), and 6.38–6.40 (m, 2H).

*Methyl 1-(3-cyanobenzyl)-5,5-dimethyl-2-oxopyrrolidine-3-carboxylate (8h)*. ^{1}H-NMR (CDCl$_3$, 400 MHz, significant signals from a 2:1 mixture of **8h** and *cis-***7h**) δ 1.16 (s, 3H), 1.24 (s, 3H), 2.19 (dd, *J* = 12.8 and 9.2 Hz, 1H), 2.33 (dd, *J* = 12.8 and 9.2 Hz, 1H), 3.62 (t, *J* = 9.2 Hz, 1H), 3.80 (s, 3H), 4.33 (d, *J* = 16.0 Hz, 1H), and 4.55 (d, *J* = 16.0 Hz, 1H).

*Methyl 2-tert-butyl-8-methoxy-3-oxo-1H-2,3-dihydrocyclohepta[c]pyrrole-3a-carboxylate (6i)*. ^{1}H-NMR (CDCl$_3$, 400 MHz, signals from a 1.5:1 mixture of **6i** and *cis-***7i**) δ 1.47 (s, 9H), 3.55 (s, 3H), 3.69 (s, 3H), 4.23 (dd, *J* = 14.4 and 1.6 Hz, 1H), 4.48 (dd, *J* = 14.4 and 1.6 Hz, 1H), 5.65 (d, *J* = 7.2 Hz, 1H), 6.29–6.33 (m, 1H), 6.31 (d, *J* = 7.6 Hz, 1H), and 6.38–6.45 (m, 1H). ^{13}C-NMR (CDCl$_3$, 100.6 MHz, significant signals from a 1:8 mixture of **6i** and *cis-***7i**) δ 27.6 (3 CH$_3$), 49.4 (CH$_2$), 52.8 (CH$_3$), 55.1 (C), 57.5 (CH$_3$), 99.8 (CH), 120.6 (CH), 122.5 (CH), and 126.9 (CH).

*Methyl 1-(2-fluorobenzyl)-5,5-dimethyl-2-oxopyrrolidine-3-carboxylate (8j)*. ^{1}H-NMR (CDCl$_3$, 400 MHz, signals from a 8:1 mixture of **8j** and *cis-***7j**) δ 1.14 (s, 3H), 1.25 (s, 3H), 2.15 (dd, *J* = 12.8 and 9.2 Hz, 1H), 2.31 (dd, *J* = 12.8 and 9.2 Hz, 1H), 3.61 (t, *J* = 9.2 Hz, 1H), 3.82 (s, 3H), 4.46 (d, *J* = 16.0 Hz, 1H), 4.55 (d, *J* = 16.0 Hz, 1H), 7.00 (ddd, *J* = 10.4, 8.4, and 1.2 Hz, 1H), 7.09 (td, *J* = 7.6 and 1.2 Hz, 1H), 7.19–7.25 (m, 1H), and 7.39 (td, *J* = 7.6 and 1.2 Hz, 1H).

*Methyl 1-(2-bromobenzyl)-5,5-dimethyl-2-oxopyrrolidine-3-carboxylate (8k).* Amorphous orange solid. ^{1}H-NMR (CDCl$_3$, 400 MHz) δ 1.18 (s, 3H), 1.23 (s, 3H), 2.20 (dd, *J* = 12.8 and 9.2 Hz, 1H), 2.35 (dd, *J* = 12.8 and 9.2 Hz, 1H), 3.65 (t, *J* = 9.2 Hz, 1H), 3.83 (s, 3H), 4.45 (d, *J* = 16.4 Hz, 1H), 4.64 (d, *J* = 16.4 Hz, 1H), 7.10 (ddd, *J* = 8.0, 6.8 and 2.4 Hz, 1H), 7.24–7.30 (m, 2H), 7.51 (dd, *J* = 7.6 and 1.2 Hz, 1H). ^{13}C-NMR (CDCl$_3$, 100.6 MHz) δ 26.9 (s, CH$_3$), 27.8 (s, CH$_3$), 38.3 (CH$_2$), 43.1 (CH$_2$), 47.6 (CH), 52.9 (CH$_3$), 60.0 (C), 122.6 (C), 128.0 (CH), 128.9 (CH), 129.2 (CH), 132.7 (CH), 137.1 (C), 170.1 (C), and 171.1 (C).

*Methyl 1-(2-iodobenzyl)-5,5-dimethyl-2-oxopyrrolidine-3-carboxylate (8l).* Amorphous orange solid. ^{1}H-NMR (CDCl$_3$, 400 MHz) δ 1.20 (s, 3H), 1.22 (s, 3H), 2.20 (dd, *J* = 13.2 and 9.2 Hz, 1H), 2.35 (dd, *J* = 13.2 and 9.2 Hz, 1H), 3.65 (t, *J* = 9.2 Hz, 1H), 3.83 (s, 3H), 4.35 (d, *J* = 16.4 Hz, 1H), 4.59 (d, *J* = 16.4 Hz, 1H), 6.93 (td, *J* = 8.0 and 1.6 Hz, 1H), 7.23 (dd, *J* = 8.0 and 1.6 Hz, 1H), 7.30 (td, *J* = 8.0 and 1.2 Hz, 1H), and 7.79 (dd, *J* = 8.0 and 1.2 Hz, 1H).

*Methyl cis-1-tert-butyl-2-oxo-4-(pyridin-4-yl)azetidine-3-carboxylate (cis-12).* ^{1}H-NMR (CDCl$_3$, 400 MHz, signals from a 2.6:1 mixture of *trans*-**12** and *cis*-**12**) δ 1.32 (s, 9H), 3.36 (s, 3H), 4.28 (d, *J* = 6.4 Hz, 1H), 4.88 (d, *J* = 6.4 Hz, 1H), 7.32-7.35 (m, 2H), and 8.61–8.65 (m, 2H). ^{13}C-NMR (CDCl$_3$, 100.6 MHz, signals from a 2.6:1 mixture of ***trans*-12** and ***cis*-12**) δ 28.2 (3 CH$_3$), 52.2 (CH$_3$), 55.4 (CH), 55.5 (C), 59.0 (CH), 121.1 (2 CH), 146.2 (C), 150.2 (2 CH), 162.5 (C), and 165.9 (C).

*Methyl trans-1-tert-butyl-2-oxo-4-(pyridin-4-yl)azetidine-3-carboxylate (trans-12).* ^{1}H-NMR (CDCl$_3$, 400 MHz) δ 1.27 (s, 9H), 3.67 (d, *J* = 2.4 Hz, 1H), 3.78 (s, 3H), 4.84 (d, *J* = 2.4 Hz, 1H), 7.33 (dd, *J* = 4.4 and 1.6 Hz, 2H), and 8.64 (dd, *J* = 4.4 and 1.6 Hz, 2H). ^{13}C-NMR (CDCl$_3$, 100.6 MHz) δ 28.2 (3 CH$_3$), 53.0 (CH$_3$), 55.2 (CH), 55.7 (C), 62.1 (CH), 121.6 (2 CH), 148.5 (C), 150.7 (2 CH), 161.7 (C), and 167.0 (C).

## 4. Computational Details

All the calculations reported in this paper were performed with the Gaussian 09 suite of programs [66]. Electron correlation was partially taken into account using the hybrid functional usually denoted as B3LYP [67–69] in conjunction with the D3 dispersion correction suggested by Grimme et al. [70] using the standard double-ζ quality def2-SVP [71,72] basis set for all atoms. The Polarizable Continuum Model (PCM) [73–75] was used to model the effects of the solvent. This level is denoted PCM(solvent)-B3LYP-D3/def2-SVP. Geometries were fully optimized in solution without any geometry or symmetry constraints. Reactants, intermediates, and products were characterized by frequency calculations and have positive definite Hessian matrices. Transition structures (TSs) show only one negative eigenvalue in their diagonalized force constant matrices, and their associated eigenvectors were confirmed to correspond to the motion along the reaction coordinate under consideration using the Intrinsic Reaction Coordinate (IRC) method [76]. Frequency calculations were also used to determine the difference between the potential (E) and Gibbs (G) energies, G − E, which contains the zero-point, thermal, and entropy energies. Potential energies were refined, E$_{sol}$, by means of single point (SP) calculations at the same level with a larger basis set, def2-TZVPP [71,72], where all elements were described with a triple-ζ plus polarization quality basis set. This level is denoted PCM(solvent)-B3LYP-D3/def2-TZVPP//PCM(solvent)-B3LYP-D3/def2-SVP. The ΔG and ΔG$^{\neq}$ values given in the text were obtained from the Gibbs energy in solution, G$_{sol}$, which was calculated by adding the thermochemistry corrections, G − E, to the refined SP energies, E$_{sol}$, i.e., G$_{sol}$ = E$_{sol}$ + G − E. See Supplementary Materials.

## 5. Conclusions

In summary, in the present paper, we report a full account of our experimental and computational studies on the Pd-catalyzed intramolecular carbene C–H insertion of α-diazo-α-(methoxycarbonyl)acetamides to prepare oxindoles and β-lactams. We have explored how the reactions are affected by the substituents on the α-diazoamide moiety and by the catalyst type, exploring the use of both Pd(0) and Pd(II) catalysts.

The chemoselectivity of the Pd-catalyzed C–H insertion reactions of α-diazo acetamides is mainly governed by the nature of the substrates. Thus, while *N*-aryl acetamides selectively afforded oxindoles, starting from *N*,*N*-dialkyl acetamides, the corresponding β-lactams were obtained.

The results obtained in the annulation reactions to form oxindoles show that Pd(0) catalysts were much more efficient than Pd(II) catalysts and that $((IMes)Pd(NQ))_2$ can be used as an alternative to $Pd_2(dba)_3$ to catalyze the carbene $C_{Ar}sp^2$–H insertion.

On the other hand, both Pd(0) and Pd(II) catalysts can be used to promote $Csp^3$–H insertion leading to β-lactams. However, the Pd(II) complexes proved to be more versatile for β-lactam formation since the use of Pd(0) catalysts resulted in increased amounts of Buchner products and, in some cases, of the corresponding γ-lactams.

Our computational studies show that when using $((IMes)Pd(NQ))_2$ as the catalyst, both $C_{Ar}sp^2$–H and $Csp^3$–H insertions involve similar stepwise reaction mechanisms, in which a palladium-mediated hydrogen migration is followed by a reductive elimination.

**Supplementary Materials:** The following are available online, Copies of $^1H$ and $^{13}C$-NMR spectra of new compounds and Cartesian coordinates and total energies of all species described in the manuscript.

**Author Contributions:** D.S. designed and planned the research; D.S. and M.-L.B. supervised the experimental work; F.P.-J. and A.A. performed the experimental work and characterized the compounds; I.F. carried out the computational studies; D.S. and I.F. prepared the manuscript for publication.

**Conflicts of Interest:** The authors declare no conflict of interest.

## References

1. Godula, K.; Sames, D. C-H Bond functionalization in complex organic synthesis. *Science* **2006**, *312*, 67–72. [CrossRef]
2. Yamaguchi, J.; Yamaguchi, A.D.; Itami, K. C-H Bond functionalization: emerging synthetic tools for natural products and pharmaceuticals. *Angew. Chem. Int. Ed.* **2012**, *51*, 8960–9009. [CrossRef]
3. Davies, H.M.L.; Manning, J.R. Catalytic C-H functionalization by metal carbenoid and nitrenoid insertion. *Nature* **2008**, *451*, 417–424. [CrossRef]
4. Doyle, M.P.; Duffy, R.; Ratnikov, M.; Zhou, L. Catalytic carbene insertion into C-H bonds. *Chem. Rev.* **2010**, *110*, 704–724. [CrossRef]
5. Zheng, C.; You, S.-L. Recent development of direct asymmetric functionalization of inert C-H bonds. *RSC Adv.* **2014**, *4*, 6173–6214. [CrossRef]
6. Ford, A.; Miel, H.; Ring, A.; Slattery, C.N.; Maguire, A.R.; McKervey, M.A. Modern organic synthesis with α-diazocarbonyl compounds. *Chem. Rev.* **2015**, *115*, 9981–10080. [CrossRef]
7. Lombard, F.J.; Coster, M.J. Rhodium(II)-catalysed intramolecular C-H insertion α- to oxygen: reactivity, selectivity and applications to natural product synthesis. *Org. Biomol. Chem.* **2015**, *13*, 6419–6431. [CrossRef]
8. Hu, F.; Xia, Y.; Ma, C.; Zhang, Y.; Wang, J. C-H bond functionalization based on metal carbene migratory insertion. *Chem. Commun.* **2015**, *51*, 7986–7995. [CrossRef]
9. Cai, Y.; Zhu, S.-F.; Wang, G.-P.; Zhou, Q.-L. Iron-catalyzed C-H functionalization of indoles. *Adv. Synth. Catal.* **2011**, *353*, 2939–2944. [CrossRef]
10. Yao, T.; Hirano, K.; Satoh, T.; Miura, M. Nickel- and cobalt-catalyzed direct alkylation of azoles with *N*-tosylhydrazones bearing unactivated alkyl groups. *Angew. Chem. Int. Ed.* **2012**, *51*, 775–779. [CrossRef]
11. Yu, Z.; Ma, B.; Chen, M.; Wu, H.-H.; Liu, L.; Zhang, J. Highly site-selective direct C-H bond functionalization of phenols with α-aryl-α-diazoacetates and diazooxindoles via gold catalysis. *J. Am. Chem. Soc.* **2014**, *136*, 6904–6907. [CrossRef]
12. Liu, X.-G.; Zhang, S.-S.; Wu, J.-Q.; Li, Q.; Wang, H. Cp*Co(III)-catalyzed direct functionalization of aromatic C-H bonds with α-diazomalonates. *Tetrahedron Lett.* **2015**, *56*, 4093–4095. [CrossRef]
13. Zhao, D.; Kim, J.H.; Stegemann, L.; Strassert, C.A.; Glorius, F. Cobalt(III)-catalyzed directed C-H coupling with diazo compounds: straightforward access towards extended π-systems. *Angew. Chem. Int. Ed.* **2015**, *54*, 4508–4511. [CrossRef]

14. Fructos, M.R.; Díaz-Requejo, M.M.; Pérez, P.J. Gold and diazo reagents: a fruitful tool for developing molecular complexity. *Chem. Commun.* **2016**, *52*, 7326–7335. [CrossRef]

15. Liu, L.; Zhang, J. Gold-catalyzed transformations of α-diazocarbonyl compounds: selectivity and diversity. *Chem. Soc. Rev.* **2016**, *45*, 506–516. [CrossRef] [PubMed]

16. Conde, A.; Sabenya, G.; Rodríguez, M.; Postils, V.; Luis, J.M.; Díaz-Requejo, M.M.; Costas, M.; Pérez, P.J. Iron and manganese catalysts for the selective functionalization of arene C(sp$^2$)-H bonds by carbene insertion. *Angew. Chem. Int. Ed.* **2016**, *55*, 6530–6534. [CrossRef] [PubMed]

17. Davies, H.M.L.; Parr, B.T. Rhodium carbenes. In *Contemporary Carbene Chemistry*; Wiley: Hoboken, NJ, USA, 2013; pp. 363–403.

18. Yakura, T.; Nambu, H. Recent topics in application of selective Rh(II)-catalyzed C-H functionalization toward natural product synthesis. *Tetrahedron Lett.* **2018**, *59*, 188–202. [CrossRef]

19. Díaz-Requejo, M.M.; Pérez, P.J. Coinage metal catalyzed C-H bond functionalization of hydrocarbons. *Chem. Rev.* **2008**, *108*, 3379–3394. [CrossRef]

20. Zhao, X.; Zhang, Y.; Wang, J. Recent developments in copper-catalyzed reactions of diazo compounds. *Chem. Commun.* **2012**, *48*, 10162–10173. [CrossRef]

21. Choi, M.K.-W.; Yu, W.-Y.; Che, C.-M. Ruthenium-catalyzed stereoselective intramolecular carbenoid C-H insertion for β- and γ-lactam formations by decomposition of α-diazoacetamides. *Org. Lett.* **2005**, *7*, 1081–1084. [CrossRef]

22. Grohmann, M.; Buck, S.; Schäffler, L.; Maas, G. Diruthenium(I,I) catalysts for the formation of β- and γ-lactams via carbenoid C-H insertion of α-diazoacetamides. *Adv. Synth. Catal.* **2006**, *348*, 2203–2211. [CrossRef]

23. Choi, M.K.-W.; Yu, W.-Y.; So, M.-H.; Zhou, C.-Y.; Deng, Q.-H.; Che, C.-M. A Non-cross-linked soluble polystyrene-supported ruthenium catalyst for carbenoid transfer reactions. *Chem. Asian J.* **2008**, *3*, 1256–1265. [CrossRef]

24. Reddy, A.R.; Zhou, C.-Y.; Guo, Z.; Wei, J.; Che, C.-M. Ruthenium-porphyrin-catalyzed diastereoselective intramolecular alkyl carbene insertion into C-H bonds of alkyl diazomethanes generated in situ from *N*-tosylhydrazones. *Angew. Chem. Int. Ed.* **2014**, *53*, 14175–14180. [CrossRef] [PubMed]

25. Nakagawa, Y.; Chanthamath, S.; Liang, Y.; Shibatomi, K.; Iwasa, S. Regio- and enantioselective intramolecular amide carbene insertion into primary C-H bonds using Ru(II)-Pheoux catalyst. *J. Org. Chem.* **2019**, *84*, 2067–2618. [CrossRef] [PubMed]

26. Solé, D.; Amenta, A.; Bennasar, M.-L.; Fernández, I. Grubbs catalysts in intramolecular carbene C(*sp$^3$*)-H insertion reactions from α-diazoesters. *Chem. Commun.* **2019**, *55*, 1160–1163. [CrossRef] [PubMed]

27. Solé, D.; Amenta, A.; Bennasar, M.-L.; Fernández, I. Pd- and Ru-Catalyzed intramolecular carbene C$_{Ar}$-H functionalization of γ-amino-α-diazoesters for the synthesis of tetrahydroquinolines. *Chem. Eur. J.* **2019**, *25*, 10239–10245. [CrossRef] [PubMed]

28. Taber, D.F.; Amedio, J.C.; Sherill, R.G. Palladium-mediated diazo insertion: Preparation of 3-alkyl-2-carbomethoxycyclopentenones. *J. Org. Chem.* **1986**, *51*, 3382–3384. [CrossRef]

29. Matsumoto, M.; Watanabe, N.; Kobayashi, H. Metal-catalyzed intramolecular cyclization of 2-diazo-4-(4-indolyl)-3-oxobutanoic acid esters. *Heterocycles* **1987**, *26*, 1479–1482. [CrossRef]

30. Rosenberg, M.L.; Aasheim, J.H.F.; Trebbin, M.; Uggerud, E.; Hansen, T. Synthesis of a 1,3,4,5-tetrahydrobenzindole β-ketoester. *Tetrahedron Lett.* **2009**, *50*, 6506–6508. [CrossRef]

31. Goll, J.M.; Fillion, E. Tuning the reactivity of palladium carbenes derived from diphenylketene. *Organometallics* **2008**, *27*, 3622–3625. [CrossRef]

32. Zhang, Y.; Wang, J. Recent developments in Pd-catalyzed reactions of diazo compounds. *Eur. J. Org. Chem.* **2011**, 1015–1026. [CrossRef]

33. Barluenga, J.; Valdés, C. Tosylhydrazones: new uses for classic reagents in palladium-catalyzed cross-coupling and metal-free reactions. *Angew. Chem. Int. Ed.* **2011**, *50*, 7486–7500. [CrossRef] [PubMed]

34. Shao, Z.; Zhang, H. *N*-Tosylhydrazones: versatile reagents for metal-catalyzed and metal-free cross-coupling reactions. *Chem. Soc. Rev.* **2012**, *41*, 560–572. [CrossRef] [PubMed]

35. Xiao, Q.; Zhang, Y.; Wang, J. Diazo compounds and *N*-tosylhydrazones: novel cross-coupling partners in transition-metal-catalyzed reactions. *Acc. Chem. Res.* **2013**, *46*, 236–247. [CrossRef] [PubMed]

36. Reiser, O. Cyclopropanation and other reactions of palladium-carbene (and carbine) complexes. In *Handbook of Organopalladium Chemistry for Organic Synthesis*; Negishi, E., Ed.; Wiley-Interscience: New York, NY, USA, 2002; Volume 1, pp. 1561–1577.

37. Gois, P.M.P.; Afonso, C.A.M. Stereo- and regiocontrol in the formation of lactams by rhodium-carbenoid C-H insertion of α-diazoacetamides. *Eur. J. Org. Chem.* **2004**, 3773–3788. [CrossRef]

38. Ring, A.; Ford, A.; Maguire, A.R. Substrate and catalyst effects in C-H insertion reactions of α-diazoacetamides. *Tetrahedron Lett.* **2016**, *57*, 5399–5406. [CrossRef]

39. Grohmann, M.; Maas, G. Ruthenium catalysts for carbenoid intramolecular C-H insertion of 2-diazoacetoacetamides and diazomalonic ester amides. *Tetrahedron* **2007**, *63*, 12172–12178. [CrossRef]

40. Large, T.; Müller, T.; Kunkel, H.; Buck, S.; Maas, G. Ruthenium- and rhodium-catalyzed carbenoid reactions of diazoesters in hexaalkylguanidinium-based ionic liquids. *Z. Naturforsch. B* **2012**, *67*, 347–353. [CrossRef]

41. Chan, W.-W.; Kwong, T.-L.; Yu, W.-Y. Ruthenium-catalyzed intramolecular cyclization of diazo-β-ketoanilides for the synthesis of 3-alkylideneoxindoles. *Org. Biomol. Chem.* **2012**, *10*, 3749–3755. [CrossRef]

42. Liu, N.; Tian, Q.-P.; Yang, Q.; Yang, S.-D. Ruthenium-catalyzed intramolecular cyclization and fluorination to form 3-fluorooxindoles. *Synlett* **2016**, *27*, 2621–2625.

43. Yamamoto, K.; Qureshi, Z.; Tsoung, J.; Pisella, G.; Lautens, M. Combining Ru-catalyzed C-H functionalization with Pd-catalyzed asymmetric allylic alkylation: synthesis of 3-allyl-3-aryl oxindoles derivatives from aryl α-diazoamides. *Org. Lett.* **2016**, *18*, 4954–4957. [CrossRef] [PubMed]

44. Merlic, C.A.; Zechman, A.L. Selectivity in rhodium(II) catalyzed reactions of diazo compounds: effects of catalyst electrophilicity, diazo substitution, and substrate substitution. From chemoselectivity to enantioselectivity. *Synthesis* **2003**, 1137–1156. [CrossRef]

45. Davies, H.M.L.; Morton, D. Guiding principles for site selective and stereoselective intermolecular C-H functionalization by donor/acceptor rhodium carbenes. *Chem. Soc. Rev.* **2011**, *40*, 1857–1869. [CrossRef]

46. DeAngelis, A.; Panish, R.; Fox, J.M. Rh-catalyzed intermolecular reactions of α-alkyl-α-diazo carbonyl compounds with selectivity over β-hydride migration. *Acc. Chem. Res.* **2016**, *49*, 115–127. [CrossRef] [PubMed]

47. Brown, D.S.; Elliott, M.C.; Moody, C.J.; Mowlem, T.J.; Marino, J.P.; Padwa, A. Ligand effects in the rhodium(II)-catalyzed reactions of α-diazoamides. Oxindole formation is promoted by the use of rhodium(II) perfluorocarboxamide catalysts. *J. Org. Chem.* **1994**, *59*, 2447–2455. [CrossRef]

48. Miah, S.; Slawin, A.M.Z.; Moody, C.J.; Sheedan, S.M.; Marino, J.P., Jr.; Semones, M.A.; Padwa, A.; Richards, I.C. Ligand effects in the rhodium(II) catalyzed reactions of diazoamides and diazoimides. *Tetrahedron* **1996**, *52*, 2489–2514. [CrossRef]

49. Solé, D.; Pérez-Janer, F.; Mancuso, R. Pd⁰-Catalyzed intramolecular α-arylation of sulfones: domino reactions in the synthesis of functionalized tetrahydroquinolines. *Chem. Eur. J.* **2015**, *21*, 4580–4584. [CrossRef]

50. Solé, D.; Pérez-Janer, F.; Zulaica, E.; Guastavino, J.F.; Fernández, I. Pd-Catalyzed α-arylation of sulfones in a three-component synthesis of 3-[2-(phenyl/methylsulfonyl)ethyl]indoles. *ACS Catal.* **2016**, *6*, 1691–1700. [CrossRef]

51. Solé, D.; Pérez-Janer, F.; García-Rodeja, Y.; Fernández, I. Exploring partners for the domino α-arylation/Michael addition reaction leading to tetrahydroquinolines. *Eur. J. Org. Chem.* **2017**, *2017*, 799–805. [CrossRef]

52. Solé, D.; Fernández, I. Controlling the ambiphillic nature of σ-arylpalladium intermediates in intramolecular cyclization reactions. *Acc. Chem. Res.* **2014**, *47*, 168–179. [CrossRef]

53. Solé, D.; Mariani, F.; Bennasar, M.-L.; Fernández, I. Palladium-catalyzed intramolecular carbene insertion into C(sp³)-H bonds. *Angew. Chem. Int. Ed.* **2016**, *55*, 6467–6470. [CrossRef] [PubMed]

54. Solé, D.; Amenta, A.; Mariani, F.; Bennasar, M.-L.; Fernández, I. Transition metal-catalysed intramolecular carbenoid C-H insertion for pyrrolidine formation by decomposition of α-diazoesters. *Adv. Synth. Catal.* **2017**, *359*, 3654–3664. [CrossRef]

55. Solé, D.; Pérez-Janer, F.; Fernández, I. Palladium-catalysed intramolecular carbenoid insertion of α-diazo-α-(methoxycarbonyl)acetanilides for oxindoles synthesis. *Chem. Commun.* **2017**, *53*, 3110–3113. [CrossRef] [PubMed]

56. Solé, D.; Pérez-Janer, F.; Bennasar, M.-L.; Fernández, I. Palladium catalysis in the intramolecular carbene C-H insertion of α-diazo-α-(methoxycarbonyl)acetamides to forma β-lactams. *Eur. J. Org. Chem.* **2018**, 4446–4455. [CrossRef]

57. Gabriele, B.; Salerno, G.; Veltri, L.; Costa, M.; Massera, C. Stereoselective synthesis of (*E*)-3-(methoxycarbonyl)methylene-1,3-dihydroindol-2-ones by palladium-catalyzed oxidative carbonylation of 2-ethynylanilines. *Eur. J. Org. Chem.* **2001**, 4607–4613. [CrossRef]

58. Kischkewitz, M.; Daniliuc, C.-G.; Studer, A. 3-Alkyl-3-cyano-oxindoles from 2-cyano-2-diazo-*N*-phenylacetamides via cyclizing carbene insertion and subsequent radical oxidation. *Org. Lett.* **2016**, *18*, 1206–1209. [CrossRef]

59. Ma, C.; Xing, D.; Hu, W. Catalyst-free halogenation of α-diazocarbonyl compounds with *N*-halosuccinimides: synthesis of 3-halooxindoles or vinyl halides. *Org. Lett.* **2016**, *18*, 3134–3137. [CrossRef]

60. Mo, S.; Xu, C.; Xu, J. Expeditious and convenient synthesis of polycyclic difluoroboron complexes of 2-oxoindoline-3-carboxamides by tandem reaction. *Adv. Synth. Catal.* **2016**, *358*, 1767–1777. [CrossRef]

61. Moody, C.J.; Miah, S.; Slawin, A.M.Z.; Mansfield, D.J.; Richards, I.C. Ligands effects in the metal catalyzed reactions of *N*-aryldiazoamides: ylide formation vs. insertion reactions. *Tetrahedron* **1998**, *54*, 9689–9700. [CrossRef]

62. Heil, M.; Hoffmeister, L.; Webber, M.; Ilg, K.; Goergens, U.; Turberg, A. Preparation of mesoionic imidazopyridines for use as insecticides. PCT Int. Appl. WO 2018192872 A1 20181025.

63. Bonardi, A.; Costa, M.; Gabriele, B.; Salerno, G.; Chiusoli, G.P. Versatile synthesis of beta-lactams, gamma-lactams or oxazolidines by palladium-catalysed oxidative carbonylation of 1-substituted prop-2-ynylamines. *Tetrahedron Lett.* **1995**, *36*, 7495–7498. [CrossRef]

64. Hosseyni, S.; Jarrahpour, A. Recent advances in β-lactam synthesis. *Org. Biomol. Chem.* **2018**, *16*, 6840–6852. [CrossRef] [PubMed]

65. Synofzik, J.; Dar'in, D.; Novikov, M.S.; Kantin, G.; Bakulina, O.; Krasavin, M. α-Acyl-α-diazoacetates in transition-metal-free β-lactam synthesis. *J. Org. Chem.* **2019**, *84*, 12101. [CrossRef] [PubMed]

66. Frisch, M.J.; Trucks, G.W.; Schlegel, H.B.; Scuseria, G.E.; Robb, M.A.; Cheeseman, J.R.; Scalmani, G.; Barone, V.; Mennucci, B.; Petersson, G.A.; et al. *Gaussian 09, Revision D.01*; Gaussian, Inc.: Wallingford, CT, USA, 2009.

67. Becke, A.D. Density-functional thermochemistry. III. The role of exact exchange. *J. Chem. Phys.* **1993**, *98*, 5648–5652. [CrossRef]

68. Lee, C.; Yang, W.; Parr, R.G. Development of the Colle-Salvetti correlation-energy formula into a functional of the electron density. *Phys. Rev. B* **1998**, *37*, 785–789. [CrossRef] [PubMed]

69. Vosko, S.H.; Wilk, L.; Nusair, M. Accurate spin-dependent electron liquid correlation energies for local spin density calculations: a critical analysis. *Can. J. Phys.* **1980**, *58*, 1200–1211. [CrossRef]

70. Grimme, S.; Antony, J.; Ehrlich, S.; Krieg, H. A consistent and accurate ab initio parametrization of density functional dispersion correction (DFT-D) for the 94 elements. *J. Chem. Phys.* **2010**, *132*, 154104–154119. [CrossRef]

71. Weigend, F.; Ahlrichs, R. Balanced basis sets of split valence, triple zeta valence and quadruple zeta valence quality for H to Rn: Design and assessment of accuracy. *Phys. Chem. Chem. Phys.* **2005**, *7*, 3297–3305. [CrossRef]

72. Weigend, F. Accurate Coulomb-fitting basis sets for H to Rn. *Phys. Chem. Chem. Phys.* **2006**, *8*, 1057–1065. [CrossRef] [PubMed]

73. Miertuš, S.; Scrocco, E.; Tomasi, J. Electrostatic interaction of a solute with a continuum. A direct utilization of ab-initio molecular potentials for the prevision of solvent effects. *Chem. Phys.* **1981**, *55*, 117–129. [CrossRef]

74. Pascual-Ahuir, J.L.; Silla, E.; Tuñón, I. GEPOL: An improved description of molecular surfaces. III. A new algorithm for the computation of a solvent-excluding surface. *J. Comp. Chem.* **1994**, *15*, 1127–1138. [CrossRef]

75. Barone, V.; Cossi, M. Quantum Calculation of Molecular Energies and Energy Gradients in Solution by a Conductor Solvent Model. *J. Phys. Chem. A* **1998**, *102*, 1995–2001. [CrossRef]

76. Gonzalez, C.; Schlegel, H.B. Reaction path following in mass-weighted internal coordinates. *J. Phys. Chem.* **1990**, *94*, 5523–5527. [CrossRef]

**Sample Availability:** Not available.